

## Microcalorimetric and infrared spectroscopic studies of $\gamma$ -Al<sub>2</sub>O<sub>3</sub> modified by tin oxides

Jianyi Shen <sup>a,b</sup>, R.D. Cortright <sup>a</sup>, Yi Chen <sup>b</sup> and J.A. Dumesic <sup>a,1</sup>

<sup>a</sup> *Department of Chemical Engineering, University of Wisconsin,  
Madison, WI 53706, USA*

<sup>b</sup> *Chemistry Department, Nanjing University, Nanjing 210008, PR China*

Received 18 January 1994; accepted 21 March 1994

Microcalorimetric and infrared spectroscopic studies of ammonia and carbon dioxide adsorption have been used to study the effects on the acid/base properties of adding tin oxide to  $\gamma$ -Al<sub>2</sub>O<sub>3</sub>. The addition of SnO<sub>2</sub> to  $\gamma$ -Al<sub>2</sub>O<sub>3</sub> decreases the number of strong acid sites (heats of ammonia adsorption higher than 140 kJ/mol), increases the number of weaker acid sites (heats from 110 to 130 kJ/mol), and decreases slightly the number of basic sites (heats of carbon dioxide adsorption from 70 to 150 kJ/mol). In contrast, the presence of SnO on  $\gamma$ -Al<sub>2</sub>O<sub>3</sub> decreases the total number of acid sites (heats of ammonia adsorption higher than 70 kJ/mol) and eliminates most of the basic sites. Infrared spectroscopy of adsorbed ammonia reveals interactions between aluminum cations and stannous ions, leading to a decrease in the strength of the Lewis acid sites associated with aluminum cations.

**Keywords:** acidity; basicity; microcalorimetry; ammonia; carbon dioxide;  $\gamma$ -Al<sub>2</sub>O<sub>3</sub>; SnO; SnO<sub>2</sub>

### 1. Introduction

Catalysts consisting of Pt and Sn supported on  $\gamma$ -Al<sub>2</sub>O<sub>3</sub> have been widely studied for reforming and dehydrogenation reactions [1–5]. For example, the addition of tin to platinum catalysts enhances the selectivity for the aromatization reactions and increases catalyst stability. Much work has been conducted regarding the chemical state and the role of tin in PtSn/Al<sub>2</sub>O<sub>3</sub> catalysts [6–12]. For example, it has been established that tin can be stabilized as Sn(II) in alumina [3,6–9], and it has been suggested that tin modifies the acidity of the alumina support [6,12].

In this present study, we have investigated the effect of tin on the acid/base property of  $\gamma$ -Al<sub>2</sub>O<sub>3</sub>. In particular, we have employed microcalorimetric measurements of the heats of ammonia and carbon dioxide adsorption to measure the number and strength of acid and base sites, respectively. In addition, we have used infrared

<sup>1</sup> To whom correspondence should be addressed.

spectroscopy to study the chemical states of these adsorbed molecules to determine the nature of the acid and base sites. In a previous work, we studied the acid/base properties of  $\gamma$ -Al<sub>2</sub>O<sub>3</sub> modified by K<sub>2</sub>O, MgO and La<sub>2</sub>O<sub>3</sub> [13].

## 2. Experimental

The surface area of the  $\gamma$ -Al<sub>2</sub>O<sub>3</sub> (Davison) studied was 200 m<sup>2</sup>/g. A sample containing about 1000  $\mu$ mol Sn per gram of  $\gamma$ -Al<sub>2</sub>O<sub>3</sub> was prepared by impregnating  $\gamma$ -Al<sub>2</sub>O<sub>3</sub> with a methanol solution of tributyltin acetate (Aldrich), followed by drying at 393 K overnight and calcining at 573 K for 2 h and 723 K for 6 h. The Sn/Al<sub>2</sub>O<sub>3</sub> sample exhibited the X-ray diffraction pattern of the initial  $\gamma$ -Al<sub>2</sub>O<sub>3</sub>, indicating that tin oxide was highly dispersed.

Mössbauer spectroscopy was used to monitor the valent states of tin following various treatment conditions. The Mössbauer spectra were collected at room temperature using an Austin Science Associates model S-600 Mössbauer spectrometer. The spectrometer was operated in constant acceleration mode with a 10 mCi single line  $\gamma$ -ray source of Ca<sup>119m</sup>SnO<sub>3</sub> (Amarsham). Detection of the  $\gamma$ -rays was achieved with a Xe–CO<sub>2</sub> proportional counter. A palladium filter was placed in the radiation beam to absorb X-rays from the source. The spectrometer was calibrated with BaSnO<sub>3</sub> and  $\beta$ -Sn standard absorbers. Isomer shifts are reported relative to BaSnO<sub>3</sub>.

Microcalorimetric studies of the adsorption of NH<sub>3</sub> and CO<sub>2</sub> at 423 K were carried out using a Tian-Calvet heat-flux apparatus, which has been described elsewhere [14]. The microcalorimeter was connected to a gas-handling and volumetric adsorption system, equipped with a Baratron capacitance manometer for precision pressure measurements. The differential heat of adsorption versus adsorbate coverage was obtained by measuring the heats evolved when doses of gas (2–5  $\mu$ mol) were admitted sequentially onto the catalyst until the surface was saturated by adsorbed species.

Ammonia was purified by successive freeze/pump/thaw cycles. Carbon dioxide with a purity of 99.99% (Anaerobe, AGA Specialty Gases & Equipment) was used without further purification. Before microcalorimetric measurements, the samples were typically dried under vacuum at 573 K for 1 h, calcined in 500 Torr O<sub>2</sub> at 723 K for 6 h and evacuated at 723 K for 1–2 h. The  $\gamma$ -Al<sub>2</sub>O<sub>3</sub> treated in this way was designated as Al<sub>2</sub>O<sub>3</sub>(O). The SnO/Al<sub>2</sub>O<sub>3</sub> sample was obtained by reducing the sample in H<sub>2</sub> at 753 K. For comparison, the  $\gamma$ -Al<sub>2</sub>O<sub>3</sub> was also treated in H<sub>2</sub> at 753 K and was designated as Al<sub>2</sub>O<sub>3</sub>(R).

Infrared spectra were collected with a Nicolet FX 7000 FTIR system equipped with a liquid-nitrogen cooled MCT detector. Each spectrum was recorded at 2 cm<sup>−1</sup> resolution with 32 co-added scans. Sample pellets were formed with a thickness of 20–30 mg/cm<sup>2</sup>. The samples were loaded into a quartz cell equipped with CaF<sub>2</sub> windows, followed by the same sample treatments used for microcalorimetric

adsorption studies. Ammonia and carbon dioxide were then dosed onto the sample at 423 K for 0.5 h. The cell was then isolated, cooled to room temperature and evacuated sequentially at 298, 373 and 473 K. Infrared spectra were collected after each evacuation.

### 3. Results and discussion

Mössbauer spectra of the  $\text{Sn}/\text{Al}_2\text{O}_3$  sample as-prepared and reduced in  $\text{H}_2$  at different temperatures are shown in fig. 1. The corresponding Mössbauer parameters are given in table 1. After calcination at 723 K for 6 h, the sample exhibited a doublet with an isomer shift of 0.06 mm/s and a quadrupole splitting of 0.91 mm/s, which can be assigned to  $\text{SnO}_2$ . Reduction of this sample in  $\text{H}_2$  at 723 K reduced 82% of the  $\text{SnO}_2$  to  $\text{SnO}$  as determined by the change of intensity of the  $\text{SnO}_2$  peak.

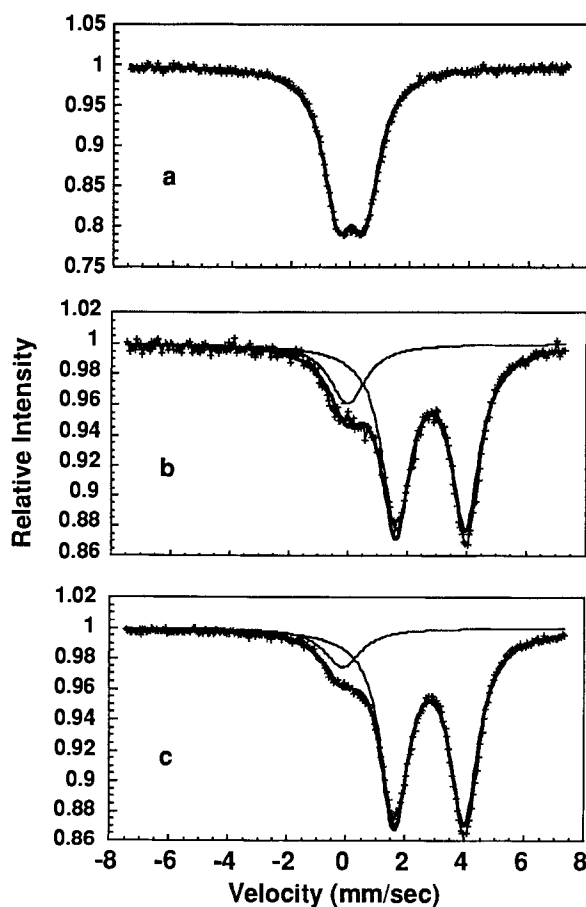


Fig. 1. Mössbauer spectra of  $\text{Sn}/\text{Al}_2\text{O}_3$  after: (a) calcination in  $\text{O}_2$  at 723 K for 6 h, (b) reduction in  $\text{H}_2$  at 723 K for 4 h, and (c) reduction in  $\text{H}_2$  at 753 K for 4 h.

Table 1

Mössbauer spectroscopy parameters of SnO<sub>2</sub>/Al<sub>2</sub>O<sub>3</sub> and SnO/Al<sub>2</sub>O<sub>3</sub> samples

Treatment	Mössbauer parameters				Assignment
	$\delta^a$ (mm/s)	$\Delta^b$ (mm/s)	width (mm/s)	area (%)	
723 K, O <sub>2</sub> , 6 h	0.06	0.91	1.18	100	SnO <sub>2</sub>
723 K, H <sub>2</sub> , 4 h	0	—	1.46	18	SnO <sub>2</sub>
	2.83	2.35	1.15	82	SnO
753 K, H <sub>2</sub> , 4 h	−0.13	—	1.49	12	SnO <sub>2</sub>
	2.83	2.35	1.15	88	SnO

<sup>a</sup>  $\delta$  = isomer shift.<sup>b</sup>  $\Delta$  = quadrupole splitting.

The peaks associated with SnO have an isomer shift of 2.83 mm/s and a quadrupole splitting of 2.35 mm/s. Bacaud et al. [6] observed similar Mössbauer parameters for SnO<sub>2</sub> and SnO on alumina. Further reduction in H<sub>2</sub> at 753 K increased the content of SnO to 88%. These Mössbauer experiments showed no indication of Sn metal (isomer shift of 2.55 mm/s) after reduction at either 723 or 753 K. Based on these Mössbauer spectroscopy results, calcination at 723 K in O<sub>2</sub> and reduction at 753 K in H<sub>2</sub> were employed to obtain samples for microcalorimetric measurements that consisted primarily of SnO<sub>2</sub> and SnO, respectively on  $\gamma$ -Al<sub>2</sub>O<sub>3</sub>.

Fig. 2 shows the differential heats of adsorption versus coverage of ammonia on  $\gamma$ -Al<sub>2</sub>O<sub>3</sub>, SnO<sub>2</sub>/Al<sub>2</sub>O<sub>3</sub>, and SnO/Al<sub>2</sub>O<sub>3</sub>. The initial heat of ammonia adsorption on  $\gamma$ -Al<sub>2</sub>O<sub>3</sub>(O) was approximately 155 kJ/mol. The addition of SnO<sub>2</sub> decreased the initial heat of ammonia adsorption to 145 kJ/mol. Moreover, SnO<sub>2</sub> decreased the strength of stronger acid sites and increased the strength of intermediate and

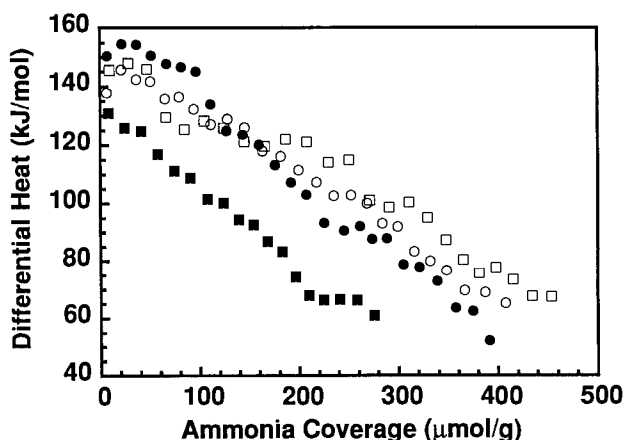


Fig. 2. Differential heat versus adsorbate coverage for adsorption of NH<sub>3</sub> at 423 K on  $\gamma$ -Al<sub>2</sub>O<sub>3</sub> calcined at 723 K (●),  $\gamma$ -Al<sub>2</sub>O<sub>3</sub> treated in H<sub>2</sub> at 753 K (○), SnO<sub>2</sub>/ $\gamma$ -Al<sub>2</sub>O<sub>3</sub> (□), and SnO/ $\gamma$ -Al<sub>2</sub>O<sub>3</sub> (■).

weak acid sites. Treatment of  $\gamma$ -Al<sub>2</sub>O<sub>3</sub> in H<sub>2</sub> at 753 K also decreased the initial heat of ammonia adsorption to about 145 kJ/mol, but the treatment did not affect sites of intermediate strength and weak acid sites on  $\gamma$ -Al<sub>2</sub>O<sub>3</sub>. The different behavior of the  $\gamma$ -Al<sub>2</sub>O<sub>3</sub>(O) and  $\gamma$ -Al<sub>2</sub>O<sub>3</sub>(R) samples is probably caused by the different temperatures employed in these treatments, i.e., 723 and 753 K, respectively. In contrast to the SnO<sub>2</sub>/Al<sub>2</sub>O<sub>3</sub> sample, the SnO/Al<sub>2</sub>O<sub>3</sub> sample showed a decrease in the total number of acid sites on  $\gamma$ -Al<sub>2</sub>O<sub>3</sub>. The initial heat of ammonia adsorption decreased from 155 to 130 kJ/mol and the total coverage of ammonia decreased from about 400  $\mu$ mol/g to less than 280  $\mu$ mol/g upon the reduction to SnO.

The microcalorimetric results of carbon dioxide adsorption on  $\gamma$ -Al<sub>2</sub>O<sub>3</sub>, SnO<sub>2</sub>/Al<sub>2</sub>O<sub>3</sub>, and SnO/Al<sub>2</sub>O<sub>3</sub> are shown in fig. 3. The initial heat of CO<sub>2</sub> adsorption on  $\gamma$ -Al<sub>2</sub>O<sub>3</sub> was about 145 kJ/mol. The addition of SnO<sub>2</sub> decreased the heat of CO<sub>2</sub> adsorption on essentially all base sites and decreased the saturation CO<sub>2</sub> coverage from 80 to 55  $\mu$ mol/g. Treatment of  $\gamma$ -Al<sub>2</sub>O<sub>3</sub> in H<sub>2</sub> at 753 K did not influence the subsequent adsorption of CO<sub>2</sub>. However, the presence of SnO significantly decreased the basicity of  $\gamma$ -Al<sub>2</sub>O<sub>3</sub>. The initial heat of CO<sub>2</sub> adsorption decreased from 145 to 110 kJ/mol, and the saturation CO<sub>2</sub> coverage decreased from 80 to 25  $\mu$ mol/g.

Fig. 4 shows histograms of the apparent distribution of site strengths for ammonia and carbon dioxide adsorption on  $\gamma$ -Al<sub>2</sub>O<sub>3</sub>, SnO<sub>2</sub>/Al<sub>2</sub>O<sub>3</sub>, and SnO/Al<sub>2</sub>O<sub>3</sub>. The histograms were obtained by first fitting the data of differential heat versus coverage by a polynomial and then using the fitted polynomial to determine the amount of adsorbates adsorbed within a given range of differential heats. The histograms for ammonia adsorption show that  $\gamma$ -Al<sub>2</sub>O<sub>3</sub> exhibits a wide range of heats of adsorption. The addition of SnO<sub>2</sub> decreases the number of sites with differential heat near 150 kJ/mol and increases the number of sites with differential heat near

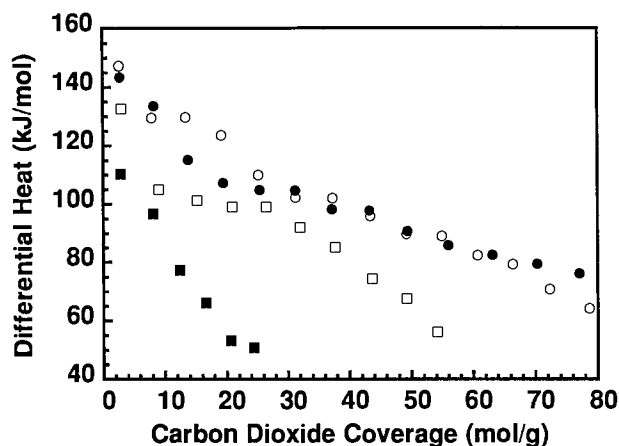


Fig. 3. Differential heat versus adsorbate coverage for adsorption of CO<sub>2</sub> at 423 K on  $\gamma$ -Al<sub>2</sub>O<sub>3</sub> calcined at 723 K (●),  $\gamma$ -Al<sub>2</sub>O<sub>3</sub> treated in H<sub>2</sub> at 753 K (○), SnO<sub>2</sub>/ $\gamma$ -Al<sub>2</sub>O<sub>3</sub> (□), and SnO/ $\gamma$ -Al<sub>2</sub>O<sub>3</sub> (■).

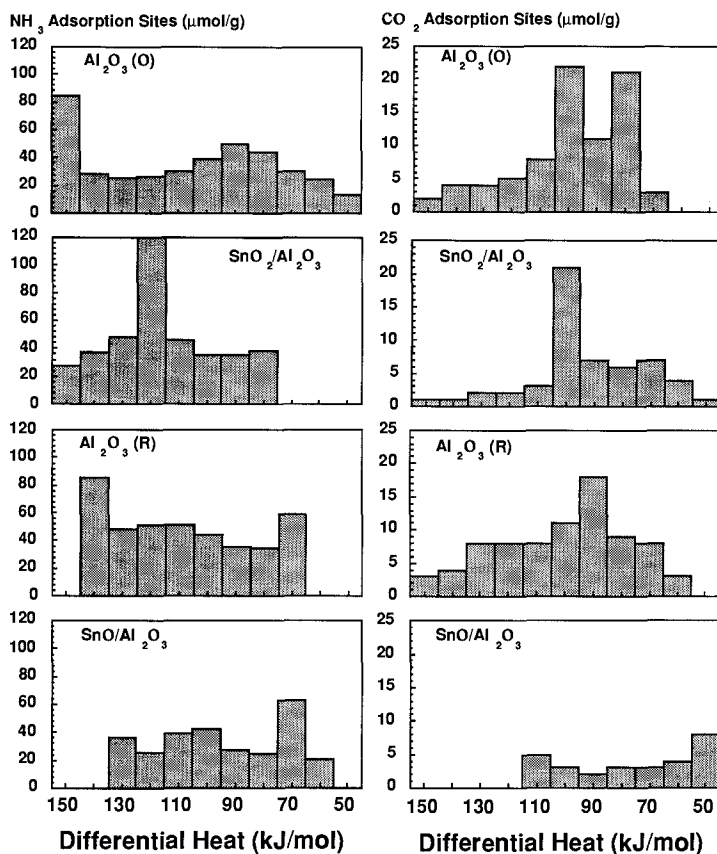


Fig. 4. Histograms of the apparent distribution of site strengths for  $\text{NH}_3$  and  $\text{CO}_2$  adsorption on  $\gamma$ - $\text{Al}_2\text{O}_3$ ,  $\text{SnO}_2/\gamma$ - $\text{Al}_2\text{O}_3$  and  $\text{SnO}/\gamma$ - $\text{Al}_2\text{O}_3$ .

120 kJ/mol. Treatment of alumina in  $\text{H}_2$  at 753 K eliminated sites with differential heat near 150 kJ/mol and slightly narrowed the site distribution. The presence of  $\text{SnO}$  eliminated sites with differential heat higher than 140 kJ/mol and significantly decreased the number of sites with heats higher than 70 kJ/mol.

The histograms of fig. 4 for  $\text{CO}_2$  adsorption indicate that basic sites of  $\gamma$ - $\text{Al}_2\text{O}_3$  show differential heats from 70 to 150 kJ/mol. The addition of  $\text{SnO}_2$  significantly decreased the number of  $\text{CO}_2$  adsorption sites over the entire range of heats; however, a considerable number of sites remained near 100 kJ/mol. Treatment of  $\gamma$ - $\text{Al}_2\text{O}_3$  in  $\text{H}_2$  at 753 K had little effect on the basic sites. The  $\text{SnO}/\text{Al}_2\text{O}_3$  sample possessed very few basic sites, and the sites present showed differential heats lower than 110 kJ/mol.

Fig. 5 shows IR spectra collected after exposure of  $\gamma$ - $\text{Al}_2\text{O}_3$ ,  $\text{SnO}_2/\text{Al}_2\text{O}_3$ , and  $\text{SnO}/\text{Al}_2\text{O}_3$  to ammonia at 423 K. The bands at 1620 and 1245  $\text{cm}^{-1}$  for the spectrum of  $\text{NH}_3$  on  $\gamma$ - $\text{Al}_2\text{O}_3$  can be assigned to asymmetric and symmetric deformations, respectively, of  $\text{NH}_3$  coordinated to aluminum cations, revealing Lewis acid

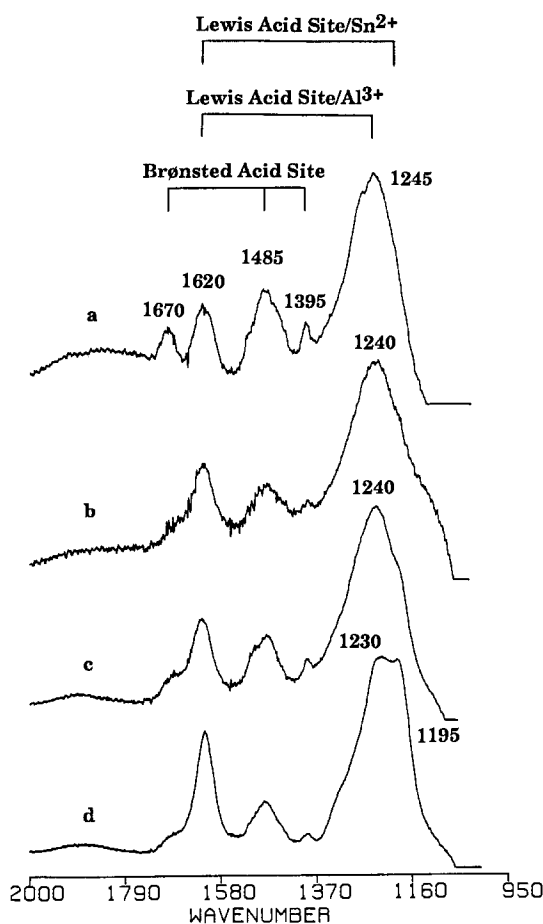


Fig. 5. Infrared spectra for ammonia adsorption at 423 K and subsequent evacuation at 298 K on  $\gamma$ - $\text{Al}_2\text{O}_3$ (O) (a),  $\text{SnO}_2/\gamma$ - $\text{Al}_2\text{O}_3$  (b),  $\gamma$ - $\text{Al}_2\text{O}_3$ (R) (c) and  $\text{SnO}/\gamma$ - $\text{Al}_2\text{O}_3$  (d).

sites [15,16]. The bands at 1700, 1485 and  $1395\text{ cm}^{-1}$  are attributed to  $\text{NH}_4^+$  species formed by the interaction of  $\text{NH}_3$  with Brønsted acid sites [15,16]. The  $\text{SnO}_2/\text{Al}_2\text{O}_3$  sample shows a similar IR spectrum to that of  $\gamma$ - $\text{Al}_2\text{O}_3$ , except that the relative intensities of the bands due to  $\text{NH}_4^+$  species have decreased. Treatment of  $\gamma$ - $\text{Al}_2\text{O}_3$  in  $\text{H}_2$  at 753 K also decreased the intensities of the bands for  $\text{NH}_4^+$  species, indicating that this thermal treatment decreased by the number of Brønsted acid sites. The presence of SnO on the  $\gamma$ - $\text{Al}_2\text{O}_3$  had the three following effects on the IR spectrum of adsorbed ammonia: (i) the relative intensity of the bands due to  $\text{NH}_4^+$  species decreased significantly, (ii) the band due to  $\text{NH}_3$  coordinated to Lewis acid sites shifted from 1425 to  $1230\text{ cm}^{-1}$ , and (iii) a new band appeared at  $1195\text{ cm}^{-1}$ .

The above IR results reveal a strong interaction between SnO and  $\gamma$ - $\text{Al}_2\text{O}_3$ . Davydov showed that the symmetric band of coordinately adsorbed  $\text{NH}_3$  is sensitive to the environment of the cations forming the Lewis acid site [16]. Specifically,

the frequency of this band increases with an increase in the valence of the cations. For SnO<sub>2</sub>, this band appears in the range of 1240–1250 cm<sup>-1</sup>, which is in the same range as for  $\gamma$ -Al<sub>2</sub>O<sub>3</sub>. This similarity explains why the IR spectrum of SnO<sub>2</sub>/Al<sub>2</sub>O<sub>3</sub> was similar to that of  $\gamma$ -Al<sub>2</sub>O<sub>3</sub>. Davydov et al. [16] found that the symmetric band of coordinately adsorbed NH<sub>3</sub> was in the range of 1240–1255 cm<sup>-1</sup> on oxidized Sn–Mo–O and Sn–V–O catalysts, similar to the range over SnO<sub>2</sub>. For a reduced sample with Sn/Mo = 9 : 1, they found two frequencies at 1210 and 1190 cm<sup>-1</sup>. Therefore, we assign the band at 1230 cm<sup>-1</sup> for the SnO/Al<sub>2</sub>O<sub>3</sub> sample to NH<sub>3</sub> coordinately adsorbed on aluminum cations, and the band at 1195 cm<sup>-1</sup> may be attributed to NH<sub>3</sub> coordinately adsorbed on Sn<sup>2+</sup> cations. The aluminum cations involved in this Lewis acid site appear to be interacting with the Sn<sup>2+</sup> cations, since the frequency of the band (1230 cm<sup>-1</sup>) was significantly lower than that for  $\gamma$ -Al<sub>2</sub>O<sub>3</sub> (1245 cm<sup>-1</sup>). The shift of this band to lower frequency suggests a decrease of partial charges on aluminum cations caused by the interaction with Sn<sup>2+</sup> cations, thereby decreasing the strength of Lewis acid sites. This conclusion is consistent with the microcalorimetric results of ammonia adsorption. The IR spectra for ammonia adsorption on the SnO/ $\gamma$ -Al<sub>2</sub>O<sub>3</sub> sample after evacuation at 373 and 473 K support the assignments. Specifically, the intensity of the band near 1195 cm<sup>-1</sup> decreased faster than the band near 1230 cm<sup>-1</sup> upon heating in vacuum, indicating that the Lewis acid sites associated with Sn<sup>2+</sup> cations were weaker than those associated with aluminum cations.

Fig. 6 shows IR spectra collected after exposure of  $\gamma$ -Al<sub>2</sub>O<sub>3</sub>, SnO<sub>2</sub>/Al<sub>2</sub>O<sub>3</sub>, and SnO/Al<sub>2</sub>O<sub>3</sub> to carbon dioxide at 423 K. The spectra for CO<sub>2</sub> on Al<sub>2</sub>O<sub>3</sub> and SnO<sub>2</sub>/Al<sub>2</sub>O<sub>3</sub> were very similar. The bands near 1650, 1480 and 1235 cm<sup>-1</sup> are due to bicarbonate species formed by the adsorption of CO<sub>2</sub> on hydroxyl groups [17,18], and bands near 1460 and 1090 cm<sup>-1</sup> may be assigned to free carbonate ions [17–19]. Thornton et al. studied CO<sub>2</sub> adsorption on SnO<sub>2</sub> with IR spectroscopy and also observed the formation of carbonate and bicarbonate species [20]. Fig. 7 shows that all these bands are essentially eliminated on the SnO/Al<sub>2</sub>O<sub>3</sub> sample, in agreement with the microcalorimetric result.

Bacaud et al. [6] also observed that addition of tin poisoned the stronger acidic sites of alumina. Over a catalyst with 0.47 wt% Pt and 0.47 wt% Sn (comparable to industrial Pt/Sn reforming catalysts), these authors observed that the addition of tin decreased the cracking activity of *n*-heptane at 673 K. Mössbauer spectroscopic studies indicated the presence of stannic and stannous cations associated with the alumina support, as well as Pt/Sn alloy species, and these authors attributed the decreased cracking activity to the elimination by tin species of the stronger acid sites on alumina.

Figs. 7 and 8 give comparisons of the effects on the acid/base properties of adding SnO<sub>2</sub> and SnO to  $\gamma$ -Al<sub>2</sub>O<sub>3</sub> with data presented elsewhere for the effects of adding K<sub>2</sub>O, MgO and La<sub>2</sub>O<sub>3</sub> [13]. It can be seen in fig. 7 that the effect of SnO on the acidity of  $\gamma$ -Al<sub>2</sub>O<sub>3</sub> was similar to that of MgO at low ammonia coverage. At higher ammonia coverages, the differential heat of ammonia adsorption on the sample



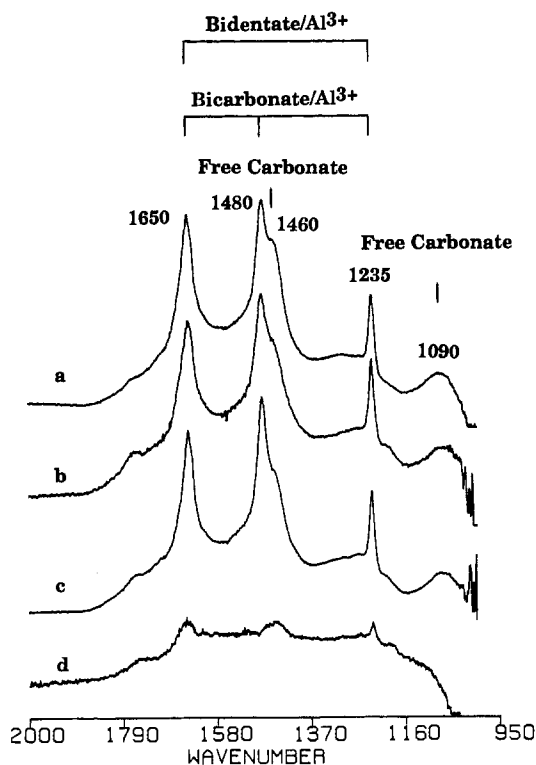


Fig. 6. Infrared spectra for carbon dioxide adsorption at 423 K and subsequent evacuation at 298 K on  $\gamma$ - $\text{Al}_2\text{O}_3$  (O) (a),  $\text{SnO}/\gamma$ - $\text{Al}_2\text{O}_3$  (b),  $\gamma$ - $\text{Al}_2\text{O}_3$  (R) (c) and  $\text{SnO}/\gamma$ - $\text{Al}_2\text{O}_3$  (d).

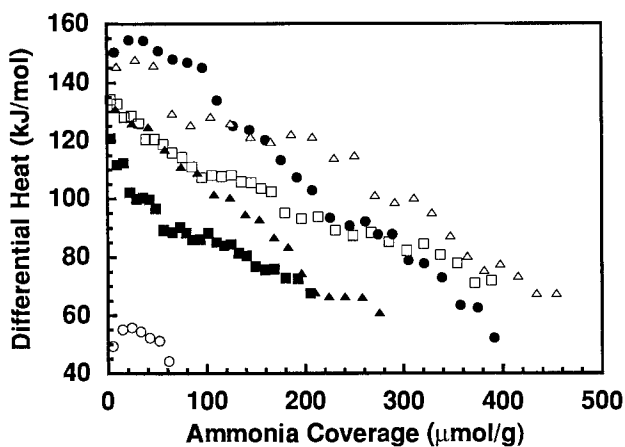


Fig. 7. Differential heat versus adsorbate coverage for adsorption of  $\text{NH}_3$  at 423 K on  $\gamma$ - $\text{Al}_2\text{O}_3$  (●) and  $\gamma$ - $\text{Al}_2\text{O}_3$  containing oxides of 3000  $\mu\text{mol K}^+/\text{g}$  (○), 3000  $\mu\text{mol Mg}^{2+}/\text{g}$  (□), 3000  $\mu\text{mol La}^{3+}/\text{g}$  (■), 1000  $\mu\text{mol Sn}^{2+}/\text{g}$  (▲), and 1000  $\mu\text{mol Sn}^{4+}/\text{g}$  (△).

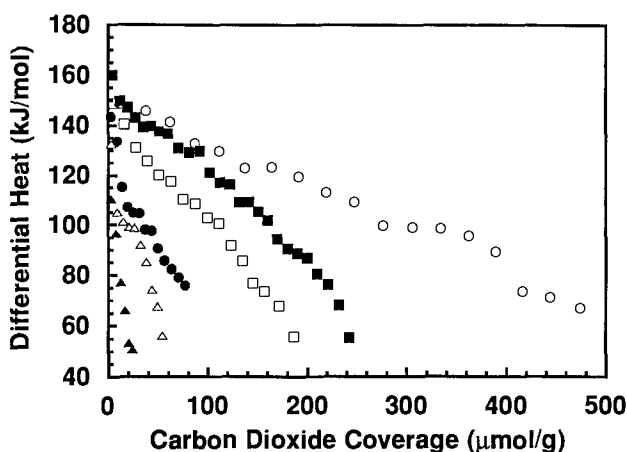
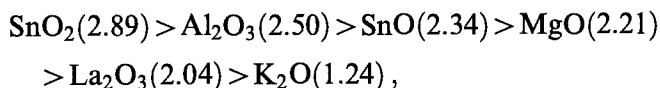


Fig. 8. Differential heat versus adsorbate coverage for adsorption of  $\text{CO}_2$  at 423 K on  $\gamma$ - $\text{Al}_2\text{O}_3$  (●) and  $\gamma$ - $\text{Al}_2\text{O}_3$  containing oxides of  $3000 \mu\text{mol K}^+/\text{g}$  (○),  $3000 \mu\text{mol Mg}^{2+}/\text{g}$  (□),  $3000 \mu\text{mol La}^{3+}/\text{g}$  (■),  $1000 \mu\text{mol Sn}^{2+}/\text{g}$  (▲), and  $1000 \mu\text{mol Sn}^{4+}/\text{g}$  (△).

containing SnO was considerably lower than that of  $\text{MgO}/\text{Al}_2\text{O}_3$ . Thus, it appears that SnO is more effective in eliminating acid sites on  $\gamma$ - $\text{Al}_2\text{O}_3$  than is MgO. It can be seen in fig. 8 that all the basic metal oxides increased the basicity of  $\gamma$ - $\text{Al}_2\text{O}_3$ . In contrast, the presence of SnO decreased the basicity of the support. Thus, SnO is the most effective oxide of those that we have studied for neutralization of the acid/base properties of  $\gamma$ - $\text{Al}_2\text{O}_3$ . Moreover, this system offers the unique ability to restore most of the acid and base sites on  $\gamma$ - $\text{Al}_2\text{O}_3$  by oxidizing the SnO to  $\text{SnO}_2$ .

We noted in our previous study of  $\text{K}_2\text{O}$ , MgO, and  $\text{La}_2\text{O}_3$  on  $\gamma$ - $\text{Al}_2\text{O}_3$  that the electronegativities of these oxides could be used to correlate the effects of these oxides on the surface acid/base properties [13]. In particular, oxides with lower electronegativities were more effective in neutralizing acid sites of alumina and generating new basic sites. We may now attempt to correlate the results in figs. 7 and 8 by ranking the oxides in the following order of decreasing electronegativity:



where the Sanderson electronegativities of the oxides are given in parentheses [21]. This ranking is in agreement with the result that  $\text{SnO}_2$  does not significantly alter the acidity of  $\text{Al}_2\text{O}_3$ , whereas SnO decreases the acidity of  $\text{Al}_2\text{O}_3$  in a manner similar to the effect of MgO. This ranking of oxides is also consistent with the observation that  $\text{SnO}_2$  decreases the basicity of  $\text{Al}_2\text{O}_3$ ; however, it does not explain the fact that SnO is even more effective than  $\text{SnO}_2$  in decreasing the basicity of  $\text{Al}_2\text{O}_3$ . We may suggest in this case that the Sn–O bond is stronger in the reduced oxide, thereby decreasing the availability of oxygen to bond with  $\text{CO}_2$ . Thus, it appears that oxidation state as well as electronegativity may be important in controlling the surface acid/base properties.

## 4. Conclusion

The additions of SnO<sub>2</sub> and SnO to  $\gamma$ -Al<sub>2</sub>O<sub>3</sub> have significantly different effects on the surface acid/base properties. Specifically, SnO<sub>2</sub> decreases the number of strong acid sites, increases the number of weaker acid sites, and has little effect on types of acid and base sites. However, the presence of SnO on  $\gamma$ -Al<sub>2</sub>O<sub>3</sub> caused a considerable decrease in the strength and number of acid sites, weakened Lewis acid sites associated with aluminum cations, and eliminated the basicity of the support. Thus, SnO is effective for neutralization of the acid/base properties of  $\gamma$ -Al<sub>2</sub>O<sub>3</sub>, this system offers the unique ability to restore most of the acid and base sites on  $\gamma$ -Al<sub>2</sub>O<sub>3</sub> by oxidizing the SnO to SnO<sub>2</sub>.

## Acknowledgement

This work was supported by the Office of Basic Energy Sciences of the Department of Energy and through a Joint China–US Cooperative Research Grant administered by the National Science Foundation.

## References

- [1] B.H. Davis, G.A. Westfall, J. Watkins and J.J. Pezzanite, *J. Catal.* 42 (1976) 247.
- [2] F.M. Dautzenberg, J.N. Helle, P. Biloen and W.M.H. Sachtler, *J. Catal.* 63 (1980) 119.
- [3] R. Burch, *J. Catal.* 71 (1981) 348.
- [4] R. Burch and L.C. Garla, *J. Catal.* 71 (1981) 360.
- [5] K. Balakrishnan and J. Schwank, *J. Catal.* 132 (1991) 451.
- [6] R. Bacaud, P. Bussiere and F. Figueras, *J. Catal.* 69 (1981) 399.
- [7] Y. Li, K.J. Klabunde and B.H. Davis, *J. Catal.* 128 (1991) 1.
- [8] B.A. Sexton, A.E. Hughes and K. Fogger, *J. Catal.* 88 (1984) 466.
- [9] H. Lieske and J. Völter, *J. Catal.* 90 (1984) 96.
- [10] S.R. Adkins and B.H. Davis, *J. Catal.* 89 (1984) 371.
- [11] G. Meitzner, G.H. Via, F.W. Lytle, S.C. Fung and J.H. Sinfelt, *J. Phys. Chem.* 92 (1988) 2925.
- [12] B.H. Davis, in: *13th North American Meeting of the Catalysis Society*, Pittsburgh 1993, B15.
- [13] J. Shen, R.D. Cortright, Y. Chen and J.A. Dumesic, *J. Phys. Chem.* (1994), submitted.
- [14] B.E. Handy, S.B. Sharma, B.E. Spiewak and J.A. Dumesic, *Meas. Sci. Technol.*, accepted (1994).
- [15] A.A. Tsyganenko, D.V. Pozdnyakov and V.N. Filimonov, *J. Mol. Structure* 29 (1975) 299.
- [16] A.A. Davydov, *Infrared Spectroscopy of Adsorbed Species on the Surface of Transition Metal Oxides* (Wiley, New York, 1990).
- [17] N.D. Parkyns, *J. Phys. Chem.* 75 (1971) 526.
- [18] G. Busca and V. Lorenzelli, *Mater. Chem.* 7 (1982) 99.
- [19] M. Kantschewa, E.V. Albano, G. Ertl and H. Knözinger, *Appl. Catal.* 8 (1983) 71.
- [20] E.W. Thornton and P.G. Harrison, *J. Chem. Soc. Faraday Trans. I* 71 (1975) 461.
- [21] J.E. Huheey, *Inorganic Chemistry: Principles of Structure and Reactivity*, 3rd Ed. (Harper and Row, New York, 1983) p. 936.